Steady-state entanglement scaling in open quantum systems: A comparison between several master equations

Antonio D'Abbruzzo[*1],Davide Rossini[2], Vittorio Giovannetti[3], Vincenzo Alba[2]

1 Scuola Normale Superiore, 56126 Pisa, Italy
2 Scuola Normale Superiore, NEST, and Istituto Nanoscienze-CNR, 56126 Pisa, Italy
3 Dipartimento di Fisica dell' Università di Pisa and INFN, Sezione di Pisa, I-56127 Pisa, Italy

Abstract

We investigate the scaling of the fermionic logarithmic negativity (FLN) between complementary intervals in the steady state of a driven-dissipative tight-binding critical chain, coupled to two thermal reservoirs at its edges. We compare the predictions of three different master equations, namely a global Lindblad equation, the Redfield equation, and the recently proposed universal Lindblad equation (ULE). Within the global Lindblad equation approach, the FLN grows logarithmically with the subsystem size ℓ, for any value of the system-bath coupling and of the bath parameters. This is consistent with the logarithmic scaling of the mutual information analytically demonstrated in [Phys. Rev. B 106, 235149 (2022)]. In the ultraweak-coupling regime, the steady-state FLN obtained from the Redfield equation and the ULE increases logarithmically as $\mathscr{E} \propto \widetilde{c}\ln(\ell)$. The prefactor $\widetilde{c}$ is nonuniversal, and it is the same as in the global Lindblad equation. Such behavior holds even when moving to moderately weak coupling and intermediate values of ℓ. However, when venturing beyond this regime, the FLN crosses over to superlogarithmic scaling for both the Redfield equation and the ULE.

1 Introduction

Understanding how genuine quantum properties of out-of-equilibrium many-body systems are affected by an external environment [1, 2] is of paramount importance from a fundamental point of view and is also relevant for a number of modern applications, such as quantum computation [3], quantum thermodynamics [4], and quantum chemistry [5]. Here we are interested in understanding how entanglement [6–9], which is the distinctive feature of quantum mechanics, and its large-scale behavior are affected by unavoidable external disturbances [10].

The scaling of entanglement has been investigated extensively in out-of-equilibrium *closed* quantum many-body systems, where one typically observes a robust growth of entanglement with time, or when increasing the size of the region of interest. For example, in integrable systems the entanglement dynamics can be described using a hydrodynamic picture in terms of well-defined quasiparticles [11–17]: in this case, the steady state exhibits volume-law entanglement entropy, which reflects the extensive character of the thermodynamic entropy. This is accompanied by an area-law scaling for the mutual information and the logarithmic negativity [14, 18, 19], which is consistent with the expected area-law mutual information that is found in thermal states [20]. Mild area-law violations, such as logarithmic ones, have been observed in steady states arising after quantum quenches in one-dimensional systems (see Ref. [21] for a recent result).

In *open* quantum many-body systems it is more challenging to quantify entanglement. First, since the global state of the system is mixed, neither the von Neumann entropy nor the mutual information are proper measures of entanglement [22]. In this situation, one can employ the logarithmic negativity [23–25]. Moreover, a general technique for handling the dynamics of open quantum systems is still missing, and one has to resort to approximations, which typically involve a weak-coupling assumption that leads to the so-called Lindblad equation [1]. The hydrodynamic description of entanglement-related quantities has been applied to the Lindblad framework, at least for quadratic master equations in the presence of global dissipation [26–30]. Very recently, these results have been extended to describe the dynamics of the logarithmic negativity [31, 32]. Still, in the presence of global system-environment interaction, the steady-state entanglement content is modest, since the negativity exhibits an exponential approach with time to a steady-state area law. The scenario is somewhat different in the presence of localized dissipation [33–37], which can act as sources of entanglement.

Recently, in Ref. [38] it was shown that boundary-driven free-fermion chains [39] that give rise to current-carrying steady states can exhibit area-law violations of entanglement (see also Ref. [40] for a similar result). Specifically, it was shown analytically that the steady-state mutual information between two complementary regions exhibits logarithmic growth with the size, as long as the bulk of the system is tuned to the ground-state critical point. This resembles the analogue ground-state entanglement scaling, even though with a nonuniversal prefactor of the logarithmic growth, which depends on the bath parameters. Ref. [38] provided numerical evidence that a similar logarithmic growth holds for the fermionic logarithmic negativity (FLN): this signals that the steady state possesses nontrivial entanglement content, at least within the framework of the Lindblad equation and for models that can be mapped to a free-fermion ones. Similar results were obtained in Ref. [41], which demonstrated logarithmic entanglement scaling in a steady-state ensemble similar to the one arising in the setup of Ref. [38].

While master equations for the description of open quantum systems have been studied extensively in the context of few-body systems, systematic benchmarks for many-body systems are more challenging to design. The master equation employed in Ref. [38] takes the Lindblad form, with Lindblad operators that are constructed from the eigenstates of the system and thus are nonlocal in space [42]. Its microscopic derivation, besides the usual assumptions of weak coupling and Markovianity, relies on the so-called secular approximation: it requires the system-bath coupling to be small, compared to the level spacing of the system Hamiltonian spectrum [1, 2]. Secular master equations have been successfully applied over the decades in a variety of settings, most notably in quantum optics. However, since in a quantum many-body system the level spacing typically decays exponentially with size, the validity of the secular approximation can become questionable. As a consequence, a considerable amount of research has been recently devoted to build nonsecular master equations. Arguably, the most prominent example of nonsecular master equation is the Redfield equation [1, 43], even though it has an important limitation: it does not necessarily lead to a completely positive dynamics [44]. To overcome this issue, several directions have been explored, such as dynamical coarse graining [45], refined weak-coupling limit [46], partial secular approximation [47], universal Lindblad equation (ULE) [48, 49] (with precursors already appearing in Refs. [50–53]), and numerical regularization techniques [54, 55] (see also Refs. [56–60] for other approaches).

In this paper we investigate whether the steady-state entanglement scaling derived in Ref. [38], as measured by the FLN, survives beyond the framework of the global Lindblad equation. Specifically, we focus on the predictions of the Redfield equation and the ULE. Ref. [61] hinted at a possible extensive character of the mutual information in the steady

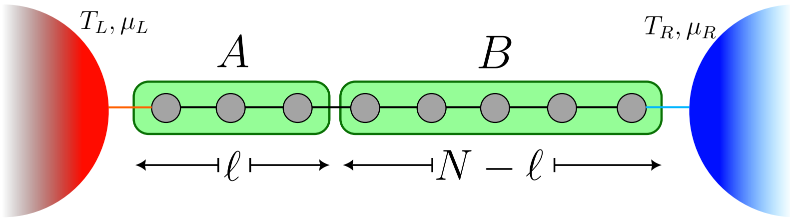

Figure 1: Setup used in this work (see Secs. 2 and 4). A fermionic chain of N sites is coupled at its edges to two fermionic thermal baths at temperatures T_L, T_R and chemical potentials μ_L, μ_R. The chain is then partitioned into the two complementary regions A and B of sizes ℓ and $N-\ell$, respectively. We are interested in the scaling of the entanglement between A and B, as measured by the FLN, in the thermodynamic limit $N, \ell \to \infty$.

state predicted by the Redfield equation, but a more thorough analysis of the behavior of the entanglement is still missing. In particular, since the mutual information is not a genuine entanglement measure, the question whether the steady state of the Redfield equation possesses nonzero entanglement remains open. We show that both the Redfield and ULE equations lead to the same steady-state logarithmic entanglement scaling, at least for intermediate-size subsystems. Interestingly, upon increasing the subsystem size, the negativity crosses over to superlogarithmic scaling: this effect is shown to be more dramatic when increasing the system-bath coupling or the difference between the chemical potentials of the baths.

The paper is structured as follows. We start with Sec. 2, where we introduce a tight-binding chain coupled to thermal baths at its edges. Sec. 3 is dedicated to the description of the Redfield equation (Sec. 3.1) and the ULE (Sec. 3.3). We also discuss how to recover the global Lindblad equation employed in Refs. [38,42] (Sec. 3.2). Then, in Sec. 4 we define the FLN as a measure of entanglement and discuss how to compute it in our setting. In Sec. 5 we discuss numerical results: in Sec. 5.1 we first introduce the employed setup, whereas in Sec. 5.2 we show that in the weak-coupling regime the three master equations give the same scaling for the steady-state negativity. In Sec. 5.3 we show that both the Redfield and the ULE exhibit superlogarithmic entanglement scaling away from the weak-coupling regime and in the thermodynamic limit. Finally, in Sec. 6 we draw our conclusions. Appendix A contains the derivation of the effective Lindblad form of the Redfield equation and the ULE used in Sec. 3.

2 Tight-binding chain with boundary driving

In this paper we consider a paradigmaitc one-dimensional quantum system $\mathcal{S}$ in contact with two thermal reservoirs at its edges (see Fig. 1). The bulk of $\mathcal{S}$ is described by a tight-binding chain Hamiltonian with open boundary conditions:

$$H_{\mathcal{S}} = -J \sum_{n=1}^{N} \left[a_n^\dagger a_{n+1} + a_{n+1}^\dagger a_n + h\, a_n^\dagger a_n \right] \tag{1}$$

with $J, h \in \mathbb{R}$ setting the energy scales of the system. Here a_n and $a_n^\dagger$ are fermionic annihilation and creation operators, satisfying

$$\{a_n, a_m^\dagger\} = \delta_{nm}, \tag{2a}$$
$$\{a_n, a_m\} = \{a_n^\dagger, a_m^\dagger\} = 0. \tag{2b}$$

The boundary conditions are imposed by requiring $a_{N+1}^{(\dagger)} \equiv 0$. We assume the initial state of the system to be quadratic in the ladder operator basis, meaning that it can be described using only even numbers of $a_n, a_n^\dagger$ operators. Moreover, in the following we measure energetic quantities in units of J, hence fixing $J = 1$. We also work in units of $\hbar = k_B = 1$.

The environment $\mathcal{E}$ consists of two free-fermionic thermal reservoirs described by the Hamiltonian $H_\mathcal{E} = H_\mathcal{E}^L + H_\mathcal{E}^R$, with

$$H_\mathcal{E}^\alpha = \sum_{r=1}^{\infty} \epsilon_{\alpha,r} c_{\alpha,r}^\dagger c_{\alpha,r}, \quad \alpha \in \{L, R\}. \tag{3}$$

The indices L and R denote the "left" and "right" baths, respectively. Here $\epsilon_{\alpha,r} \geq 0$ is the nonnegative energy of mode r of bath α, and $c_{\alpha,r}, c_{\alpha,r}^\dagger$ are fermionic annihilation and creation operators satisfying standard anticommutation relations.

Both the reservoirs are prepared in a Gaussian thermal state, each characterized by a temperature T_α and a chemical potential μ_α. The density operator $\rho_\mathcal{E}$ describing the environment is Gaussian and characterized by the correlations

$$\langle c_{\alpha,r} \rangle = \langle c_{\alpha,r}^\dagger \rangle = 0, \tag{4a}$$

$$\langle c_{\alpha,r}^\dagger c_{\beta,s} \rangle = \delta_{\alpha\beta}\, \delta_{rs}\, f_\alpha(\epsilon_{\alpha,r}), \tag{4b}$$

$$\langle c_{\alpha,r} c_{\beta,s}^\dagger \rangle = \delta_{\alpha\beta}\, \delta_{rs}\, [1 - f_\alpha(\epsilon_{\alpha,r})], \tag{4c}$$

where $\langle \cdot \rangle \coloneqq \mathrm{Tr}[\,\cdot\, \rho_\mathcal{E}]$ and $f_\alpha(x)$ is the Fermi-Dirac distribution associated with bath α, given by

$$f_\alpha(x) \coloneqq \frac{1}{1 + e^{(x-\mu_\alpha)/T_\alpha}} = \frac{1}{2}\left[1 - \tanh\left(\frac{x - \mu_\alpha}{2T_\alpha}\right)\right]. \tag{5}$$

Let us now discuss the the system-bath interaction. We consider a local interaction between the left and right reservoirs with the first and last site of the chain, respectively. We restrict ourselves system-bath Hamiltonians that are bilinear in the ladder operators of both the system and the environment as

$$H_I = X_L \otimes Y_L + X_R \otimes Y_R, \tag{6}$$

where

$$X_L = a_1 + a_1^\dagger, \quad X_R = a_N + a_N^\dagger, \tag{7a}$$

$$Y_\alpha = \sum_{r=1}^{\infty} g_{\alpha,r} \left(c_{\alpha,r} + c_{\alpha,r}^\dagger \right), \quad \alpha \in \{L, R\}, \tag{7b}$$

and $g_{\alpha,r}$ is the interaction strength associated with mode r of bath α. The bilinearity assumption will allow us to characterize the dynamics in terms of two-point correlation functions only (see Sec. 3) because the dynamics preserves the Guassianity of the system. The particular choice of Eqs. (7) is primarily dictated by their simplicity. In particular, one should observe that Eq. (7) does not preserve the fermionic number. However, particle conservation is not expected to qualitatively change the entanglement scaling, as it is clear by comparing the results of Ref. [40], which considers fermion-number preserving interactions, with those of Ref. [38]. Moreover, system-bath interactions as in Eqs. (7) were investigated previously, for instance, in Refs. [61–63]. Finally, since we assume the initial state to be quadratic in the number of ladder operators, and since in the following we will always look exclusively at two-point correlation functions, we can take X_α and Y_α

to be commuting operators, ignoring questions related to parity and how it reflects on the Hilbert space structure [64].

The total Hamiltonian is (cf. (1)(3)(6))

$$H = H_0 + H_I \equiv H_{\mathcal{S}} \otimes \mathbb{1} + \mathbb{1} \otimes H_{\mathcal{E}} + H_I, \tag{8}$$

with H_0 being the free term.

Before proceeding, we observe that the Hamiltonian $H_{\mathcal{S}}$ in Eq. (1) is straightforwardly diagonalized as [65]

$$H_{\mathcal{S}} = \sum_{k=1}^{N} E_k d_k^\dagger d_k + E_0, \tag{9}$$

where the single-particle energy dispersion E_k is

$$E_k = -h - 2\cos\left(\frac{\pi k}{N+1}\right), \tag{10}$$

while E_0 is an irrelevant constant and d_k is a fermionic annihilation operator defined by

$$a_n = \sum_{k=1}^{N} U_{nk} d_k, \quad U_{nk} = \sqrt{\frac{2}{N+1}} \sin\left(\frac{\pi n k}{N+1}\right). \tag{11}$$

From these relations, one can show that $H_{\mathcal{S}}$ exhibits ground-state criticality in the thermodynamic limit $N \to \infty$ for $|h| \leq 2$, where it is described by a conformal field theory (CFT) with central charge $c = 1$ [66, 67]. In the following, we always assume $|h| \leq 2$.

3 Treatment with Markovian master equations

Given the setting described in Sec. 2, our main goal is to describe entanglement properties of the steady state of the chain. First, one has to determine the evolution of the system density matrix $\rho(t) = \mathrm{Tr}_{\mathcal{E}}[\rho_{\mathcal{S}\mathcal{E}}(t)]$, where $\rho_{\mathcal{S}\mathcal{E}}(t)$ is the state of the chain and the environment combined. Clearly, ρ satisfies the equation

$$\frac{d\rho(t)}{dt} = -i\, \mathrm{Tr}_{\mathcal{E}}[H, \rho_{\mathcal{S}\mathcal{E}}(t)]. \tag{12}$$

As is well known, in general it is a challenging task to obtain a full solution to Eq. (12). Here we rely on the assumption of weak system-environment coupling, which is a standard procedure in the theory of open quantum systems [1, 2]. The common way of performing such approximation leads to the Redfield equation [1, 2, 43], described in Sec. 3.1. By performing the secular approximation, we derive the global Lindblad master equation in Sec. 3.2. On the other hand, in Sec. 3.3 we describe the ULE [48, 49], a recently derived completely-positive master equation that does not need the secular assumption, contrary to the Redfield equation.

3.1 Redfield master equation

At the lowest nontrivial order in the coupling between system and environment, from Eq. (12) one finds the Redfield equation [1, 2, 43]

$$\frac{d\widetilde{\rho}(t)}{dt} = \sum_{\alpha,\beta} \int_0^\infty d\tau\, C_{\alpha\beta}(\tau) [\widetilde{X}_\beta(t-\tau)\widetilde{\rho}(t), \widetilde{X}_\alpha(t)] + \mathrm{H.c.}, \tag{13}$$

where $\alpha, \beta \in \{L, R\}$ are bath indices, the tilde denotes operators in interaction picture, meaning that $\widetilde{X}(t) := e^{iH_0 t} X(t) e^{-iH_0 t}$, and

$$C_{\alpha\beta}(\tau) := \langle \widetilde{Y}_\alpha(\tau) Y_\beta \rangle \tag{14}$$

is the environment correlation function. Making use of Eqs. (4) and (7b), one obtains $C_{\alpha\beta}(\tau) = \delta_{\alpha\beta} C_\alpha(\tau)$, with

$$C_\alpha(\tau) = \int_{-\infty}^{\infty} dx\, \mathcal{J}_\alpha(x) \big\{ e^{ix\tau} f_\alpha(x) + e^{-ix\tau}[1 - f_\alpha(x)] \big\}, \tag{15}$$

where we introduced the spectral density function

$$\mathcal{J}_\alpha(x) := \sum_{r=1}^{\infty} g_{\alpha,r}^2 \delta(x - \epsilon_{\alpha,r}). \tag{16}$$

Note that, since $\epsilon_{\alpha,r} \geq 0$, we must have $\mathcal{J}_\alpha(x) = 0$ for $x < 0$.

In Appendix A we show that Eq. (13) can be written in a pseudo-Lindblad form in terms of the normal-mode Majorana operators, defined as

$$m_{2k-1} := \frac{1}{\sqrt{2}} \Big(d_k^\dagger + d_k \Big), \quad m_{2k} := \frac{i}{\sqrt{2}} \Big(d_k^\dagger - d_k \Big), \tag{17}$$

with d_k being the fermionic modes introduced in Eq. (9). Specifically, one obtains

$$\frac{d\rho(t)}{dt} = -\sum_{c,d=1}^{2N} L_{cd}[m_d m_c, \rho(t)] + \sum_{c,d=1}^{2N} M_{cd}[2 m_c \rho(t) m_d - \{m_d m_c, \rho(t)\}]. \tag{18}$$

We call this “pseudo-Lindblad form”, because it resembles the standard Lindblad form [1], even though the coefficient matrix M is not necessarily positive semidefinite. Note that the operators in Eq. (18) are not in interaction picture anymore. Here L and M are $2N \times 2N$ complex matrices such that their entries at positions $(2k-1, 2q-1)$, $(2k-1, 2q)$, $(2k, 2q-1)$, and $(2k, 2q)$, for $k, q \in \{1, \ldots, N\}$, are arranged in the 2×2 blocks $\mathcal{L}_{kq}$ and $\mathcal{M}_{kq}$ given by

$$\mathcal{L}_{kq} = \frac{1}{2} \begin{pmatrix} \mathcal{A}_{kq}^r - [\mathcal{A}_{qk}^r]^* & \delta_{kq} E_k - [\mathcal{D}_{qk}^r]^* \\ -\delta_{kq} E_k + \mathcal{D}_{kq}^r & 0 \end{pmatrix}, \tag{19a}$$

$$\mathcal{M}_{kq} = \frac{1}{2} \begin{pmatrix} \mathcal{A}_{kq}^r + [\mathcal{A}_{qk}^r]^* & [\mathcal{D}_{qk}^r]^* \\ \mathcal{D}_{kq}^r & 0 \end{pmatrix}, \tag{19b}$$

where E_k is the single-particle energy (cf. (9)). We introduced the quantities $\mathcal{A}_{kq}^r$ and $\mathcal{D}_{kq}^r$ as

$$\mathcal{A}_{kq}^r = \sum_\alpha \varphi_{\alpha,k} \varphi_{\alpha,q} [\gamma_\alpha(E_k) + \gamma_\alpha(-E_k)], \tag{20a}$$

$$\mathcal{D}_{kq}^r = i \sum_\alpha \varphi_{\alpha,k} \varphi_{\alpha,q} [\gamma_\alpha(E_k) - \gamma_\alpha(-E_k)], \tag{20b}$$

where

$$\varphi_{L,k} := U_{1,k}, \quad \varphi_{R,k} := U_{N,k}, \tag{21a}$$

$$\gamma_\alpha(\omega) := \int_0^\infty d\tau\, C_\alpha(\tau) e^{i\omega\tau}, \tag{21b}$$

with $U_{1,k}$ and $U_{N,k}$ being defined in Eq. (11). Note that, in general, $\mathcal{A}^r_{kq}$ and $\mathcal{D}^r_{kq}$ are not diagonal matrices. The system-bath interaction is encoded in γ_α in (21b). By varying γ_α, Eq. (18) allows to treat generic system bath-interactions.

Instead of working with the density matrix ρ, it is convenient to recast Eq. (18) into a differential equation for the correlation matrix G_{ab} defined as

$$G_{ab} := -i\,\mathrm{Tr}([m_a, m_b]\rho). \tag{22}$$

It is straightforward to use the adjoint of Eq. (18) to obtain the following differential continuous Lyapunov equation [68–70]:

$$\frac{dG}{dt} + PG + GP^T = Q, \tag{23}$$

where

$$P_{cd} = 2\,\mathrm{Re}[M_{cd} - L_{cd}], \quad Q_{cd} = -4\,\mathrm{Im}[M_{cd}]. \tag{24}$$

Equation (23) describes the dynamics of the Majorana operators m_{2k-1}, m_{2k} defined from the Fourier-transformed fermions d_k [cf. Eq. (17)]. However, to determine entanglement-related quantities, one has to compute the dynamics of the Majorana correlation matrix in real space, which is defined as

$$\Gamma_{ab}(\rho) := -i\,\mathrm{Tr}([w_a, w_b]\rho), \tag{25}$$

where w_a are the Majorana operators

$$w_{2n-1} := \frac{1}{\sqrt{2}}\left(a_n + a_n^\dagger\right), \quad w_{2n} := \frac{i}{\sqrt{2}}\left(a_n^\dagger - a_n\right) \tag{26}$$

defined from the original fermions $a_n, a_n^\dagger$ in Eq. (1). With a change of basis, one obtains

$$\frac{d\Gamma}{dt} + \widetilde{P}\Gamma + \Gamma\widetilde{P}^T = \widetilde{Q}, \tag{27}$$

where

$$\widetilde{P} = KPK^T, \quad \widetilde{Q} = KQK^T, \quad K = U \otimes \mathbb{1}_2. \tag{28}$$

Eq. (27) reflects that the dynamics preserved Gaussianity.

3.2 Recovering the global Lindblad equation

Before proceeding, we show how to recover the global Lindblad equation derived in Ref. [42] and employed in Ref. [38]. The global Lindblad equation relies on a secular approximation [1,2], which in the present formalism consists in neglecting all the contributions with $k \neq q$ in Eqs. (19). As a consequence, the matrices $\mathcal{A}^r_{kq}$ and $\mathcal{D}^r_{kq}$ in Eqs. (20) become diagonal and the coefficient matrices P and Q in Eq. (24) become block-diagonal as

$$P = \bigoplus_{k=1}^{N} \begin{pmatrix} 2\,\mathrm{Re}\,\mathcal{A}^r_{kk} & -E_k + 2\,\mathrm{Re}\,\mathcal{D}^r_{kk} \\ E_k & 0 \end{pmatrix}, \tag{29a}$$

$$Q = \bigoplus_{k=1}^{N} \begin{pmatrix} 0 & 2\,\mathrm{Im}\,\mathcal{D}^r_{kk} \\ -2\,\mathrm{Im}\,\mathcal{D}^r_{kk} & 0 \end{pmatrix}. \tag{29b}$$

The Lyapunov equation (23) can then be solved explicitly. In the steady state, where $dG/dt = 0$, one can use the ansatz

$$G = \bigoplus_{k=1}^{N} \begin{pmatrix} 0 & z_k \\ -z_k & 0 \end{pmatrix}, \tag{30}$$

which leads to

$$z_k = \frac{\operatorname{Im}\mathcal{D}^r_{kk}}{\operatorname{Re}\mathcal{A}^r_{kk}} = \frac{\sum_\alpha \varphi^2_{\alpha,k}[\hat{C}_\alpha(E_k) - \hat{C}_\alpha(-E_k)]}{\sum_\alpha \varphi^2_{\alpha,k}[\hat{C}_\alpha(E_k) + \hat{C}_\alpha(-E_k)]}, \tag{31}$$

One can check that this is the same result discussed in Refs. [38, 42].

3.3 Universal Lindblad Equation

The so-called ULE [48, 49] in the interaction picture takes the following form

$$\frac{d\widetilde{\rho}(t)}{dt} = \sum_\alpha \int_{-\infty}^{\infty} ds \int_{-\infty}^{\infty} ds'\, \theta(s-s') g_\alpha(s-t) g_\alpha(t-s') [\widetilde{X}_\alpha(s')\widetilde{\rho}(t), \widetilde{X}_\alpha(s)] + \text{H.c.}, \tag{32}$$

where g_α is the so-called "jump" correlation function, defined as

$$g_\alpha(\tau) \coloneqq \frac{1}{\sqrt{2\pi}} \int_{-\infty}^{\infty} d\omega \sqrt{\hat{C}_\alpha(\omega)} e^{-i\omega\tau}, \tag{33}$$

In Eq. (32) we already assumed that $C_{\alpha\beta}(\tau) = \delta_{\alpha\beta} C_\alpha(\tau)$.

Similar to the Redfield equation (see Sec. 3.1), we can write Eq. (32) in Lindblad. The result, which we derive in Appendix A, is the same as Eq. (18), where now we have

$$\mathcal{L}_{kq} = \begin{pmatrix} i\operatorname{Im}\mathcal{A}^u_{kq} & \delta_{kq}E_k/2 + \operatorname{Re}\mathcal{C}^u_{kq} \\ -\delta_{kq}E_k/2 - \operatorname{Re}\mathcal{C}^u_{qk} & i\operatorname{Im}\mathcal{B}^u_{kq} \end{pmatrix}, \tag{34a}$$

$$\mathcal{M}_{kq} = \begin{pmatrix} \operatorname{Re}\mathcal{A}^u_{kq} & i\operatorname{Im}\mathcal{C}^u_{kq} \\ -i\operatorname{Im}\mathcal{C}^u_{qk} & \operatorname{Re}\mathcal{B}^u_{kq} \end{pmatrix}, \tag{34b}$$

and $\mathcal{A}^u_{kq}$, $\mathcal{B}^u_{kq}$, $\mathcal{C}^u_{kq}$ are defined as ($\sigma, \sigma' \in \{+1, -1\}$)

$$\mathcal{A}^u_{kq} = \frac{1}{2}\sum_{\sigma,\sigma'}\sum_\alpha \varphi_{\alpha,k}\varphi_{\alpha,q}\,\mathcal{I}_\alpha(\sigma E_k, \sigma' E_q), \tag{35a}$$

$$\mathcal{B}^u_{kq} = \frac{1}{2}\sum_{\sigma,\sigma'}\sum_\alpha \varphi_{\alpha,k}\varphi_{\alpha,q}\,(-\sigma\sigma')\mathcal{I}_\alpha(\sigma E_k, \sigma' E_q), \tag{35b}$$

$$\mathcal{C}^u_{kq} = \frac{i}{2}\sum_{\sigma,\sigma'}\sum_\alpha \varphi_{\alpha,k}\varphi_{\alpha,q}\,(-\sigma')\mathcal{I}_\alpha(\sigma E_k, \sigma' E_q). \tag{35c}$$

We also introduced $\mathcal{I}_\alpha(\omega, \omega')$ as

$$\mathcal{I}_\alpha(\omega,\omega') = \pi\sqrt{\hat{C}_\alpha(-\omega)\hat{C}_\alpha(\omega')} - i\mathbb{P}\int_{-\infty}^{\infty} \frac{dx}{x}\sqrt{\hat{C}_\alpha(x-\omega)\hat{C}_\alpha(x+\omega')}, \tag{36}$$

where $\mathbb{P}$ denotes the principal value. Now, the same Lyapunov equation (23) holds true. The matrices P and Q are the same as in Eq. (24) with L, M obtained from Eqs. (34). Similar to the Redfield equation, in general P and Q are not block-diagonal matrices.

4 Fermionic logarithmic negativity

Let us now consider the bipartition of the chain in two complementary connected regions A and B (see Fig. 1). The two regions correspond to the sites $\{1, \ldots, \ell\}$ and $\{\ell+1, \ldots, N\}$, respectively. We are interested in quantifying the entanglement between A and B, given the density operator ρ of the whole chain.

Crucially, due to the presence of the thermal reservoirs, the full-chain density matrix ρ is mixed. This implies that neither the von Neumann entropy nor the Rényi entropies are proper entanglement measures [22]. A popular alternative, which is instead a computable measure of entanglement, is the logarithmic negativity $\mathscr{E}$ [23]

$$\mathscr{E}(\rho, A) := \ln \operatorname{Tr} |\rho^{T_A}|, \tag{37}$$

where $|X| := \sqrt{X^\dagger X}$, and ρ^{T_A} is the partial transpose of ρ with respect to subsystem A, defined by

$$\langle e_i^{(A)} e_j^{(B)} | \rho^{T_A} | e_k^{(A)} e_q^{(B)} \rangle = \langle e_k^{(A)} e_j^{(B)} | \rho | e_i^{(A)} e_q^{(B)} \rangle \,, \tag{38}$$

for any orthonormal basis $\{ |e_i^{(A)}\rangle \}$ of A and $\{ |e_i^{(B)}\rangle \}$ of B. For free-boson systems, if ρ is a Gaussian density matrix, ρ^{T_A} remains Gaussian. This means that $\mathscr{E}$ can be computed from the covariance matrix of ρ [71]. In contrast, for free-fermion systems, this is not true anymore.

In fact, let us rewrite the Majorana correlation matrix $\Gamma(\rho)$ [cf. Eq. (25)] as

$$\Gamma(\rho) \equiv \begin{pmatrix} \Gamma^{AA}(\rho) & \Gamma^{AB}(\rho) \\ \Gamma^{BA}(\rho) & \Gamma^{BB}(\rho) \end{pmatrix} , \tag{39}$$

where Γ^{XY} is the Majorana correlation matrix where the row and column indices are restricted to subsystems X and Y, respectively. One can show that [72]

$$\rho^{T_A} = \frac{1-i}{2} O_+ + \frac{1+i}{2} O_-, \tag{40}$$

where $O_\pm$ are Gaussian operators with corresponding Majorana correlation matrices

$$\Gamma(O_\pm) \equiv \Gamma_\pm = \begin{pmatrix} -\Gamma^{AA}(\rho) & \pm i\Gamma^{AB}(\rho) \\ \pm i\Gamma^{BA}(\rho) & \Gamma^{BB}(\rho) \end{pmatrix} . \tag{41}$$

Unfortunately, as it is clear from Eq. (40), ρ^{T_A} is not Gaussian, which implies that its spectrum and the negativity cannot be computed efficiently. However, from $O_\pm$ one can define the FLN $\mathscr{E}_F$ as

$$\mathscr{E}_F(\rho, A) := \ln \operatorname{Tr} \sqrt{O_+ O_-}. \tag{42}$$

The FLN is an upper bound for the standard logarithmic negativity that is still a proper entanglement measure, and can be defined in terms of a partial time-reversal transformation of the density matrix [73–75]. Since O_+O_- is a Gaussian operator, its spectrum and $\mathscr{E}_F$ can be computed from $\Gamma_\pm$. One obtains [74]

$$\mathscr{E}_F(\rho, A) = \frac{1}{2}\left[S_{1/2}(\rho_\times) - S_2(\rho) \right], \tag{43}$$

where $S_\alpha(\rho)$ is the α-Rényi entropy

$$S_\alpha(\rho) := \frac{1}{1-\alpha} \ln \operatorname{Tr}[\rho^\alpha], \tag{44}$$

and we defined $\rho_\times = O_+O_- / \operatorname{Tr}[O_+O_-]$. Since $\rho_\times$ is Gaussian, its spectrum is obtained from the Majorana correlation matrix

$$\Gamma(\rho_\times) = -i\mathbb{1} + i(\mathbb{1} - i\Gamma_-)(\mathbb{1} - \Gamma_+\Gamma_-)^{-1}(\mathbb{1} - i\Gamma_+). \tag{45}$$

To apply Eq. (43), one can use that for a generic Gaussian state ρ, one has [76]

$$S_\alpha(\rho) = \frac{1}{1-\alpha} \sum_j \log \left[\left(\frac{1-\nu_j}{2} \right)^\alpha + \left(\frac{1+\nu_j}{2} \right)^\alpha \right], \tag{46}$$

where $\pm i\nu_j$ ($\nu_j \in \mathbb{R}$) are the eigenvalues of $\Gamma(\rho)$. The fact that the $\pm\nu_j$ are paired is due to $\Gamma(\rho)$ being a real skew-symmetric matrix.

5 Steady-state entanglement: Numerical results

In this section we numerically investigate the scaling of the FLN in the steady state of the tight binding chain connected to two termal reservoirs (see Fig. 1). Specifically, in Sec. 5.1 we discuss how to compute the steady-state negativity in our setup. Then, in Sec. 5.2 we discuss numerical results for $\mathscr{E}_F$ obtained by employing the three different master equations introduced in Sec. 3. We show that in the weak-coupling regime the FLN exhibits logarithmic scaling with the subsystem size ℓ, at least for moderate values of ℓ. Finally, in Sec. 5.3 we show that away from the weak-coupling regime, or in the limit $\ell \to \infty$, the Redfield and ULE approaches give superlogarithmic scaling, in contrast with the global Lindblad equation which always yields logarithmic increase.

5.1 Obtaining the steady-state FLN

The first step to compute the FLN is to determine the matrices P and Q in Eq. (24) [see Eqs. (19) for the Redfield equation, Eqs. (29) for the global Lindblad equation, and Eqs. (34) for the ULE]. A crucial ingredient is the spectral density (16) of the baths and the parameters μ_α, T_α of the reservoirs in (5). Here we choose for both the baths an Ohmic spectral density with Lorentz-Drude cutoff:

$$\mathcal{J}_\alpha(x) = \theta(x)\frac{\gamma x}{x^2+\Omega^2}, \quad \gamma, \Omega > 0, \tag{47}$$

where the Heaviside theta function $\theta(x)$ reflects that $\epsilon_{\alpha,r} \geq 0$, with $\epsilon_{\alpha,r}$ being the single-particle energies of the reservoirs. To guarantee the validity of the Born-Markov approximation [1,2], one typically assumes that $\gamma \ll \Omega$ [54], which corresponds to a weak-coupling regime.

Next we numerically solve the continuous Lyapunov equation (27) for the Majorana correlation matrix Γ. Here we are interested in the steady state arising at $t \to \infty$, where $d\Gamma/dt = 0$ and we are left with the matrix equation

$$\widetilde{P}\Gamma + \Gamma\widetilde{P}^T = \widetilde{Q}, \tag{48}$$

which can be solved with polynomially-scaling complexity $\mathcal{O}(N^3)$, for instance, by using the Bartels-Stewart algorithm [77]. Notice that, due to the Gaussianity of the state, the correlation matrix Γ encodes complete information about the steady state. This is not the case for interacting fermions, for which one would have to solve the master equation for ρ, with a computational cost that scales exponentially with N.

Importantly, one can prove that Eq. (48) has a unique solution (i.e., the dynamics has a unique steady state) if and only if $\widetilde{P}$ and $-\widetilde{P}^T$ do not share any eigenvalue, meaning that $\lambda_i + \lambda_j \neq 0$ for any pair of eigenvalues λ_i, λ_j of $\widetilde{P}$. We checked that this condition is verified for our system.

Once we have Γ, we obtain the FLN as described in Sec. 4. Specifically, we consider the bipartition in Fig. 1, in which region A and B correspond to the first ℓ sites and the last $N-\ell$ sites of the chain, respectively. We first determine $\Gamma_\pm$ using Eq. (41), then we calculate $\Gamma(\rho_\times)$ using Eq. (45), and finally we obtain $\mathscr{E}_F$ by spectral decomposition using Eqs. (43) and (46).

5.2 Weak-coupling regime

In Fig. 2 we start by plotting the steady-state FLN $\mathscr{E}_F$ as a function of the size ℓ of region A. We show results for $N = 1000$ sites and $h = 1.1$. We also fix the bath parameters to $T_L = 10$, $T_R = 15$, $\mu_L = 1$, and $\mu_R = 1.5$. For the spectral density in (47) we

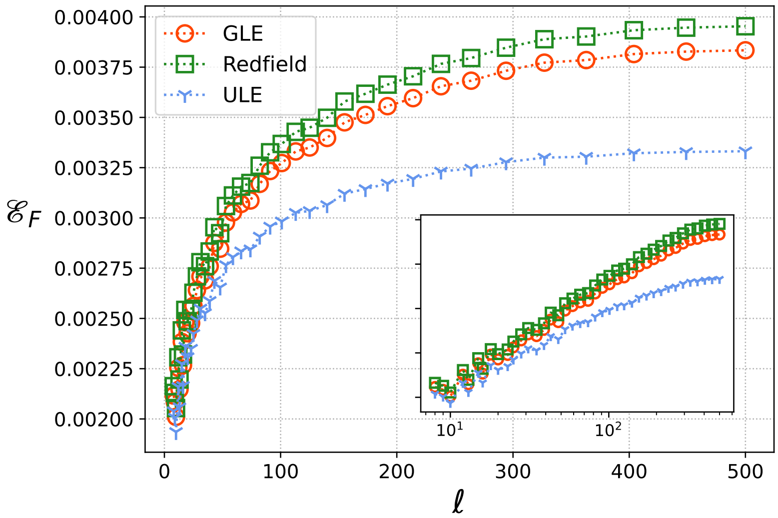

Figure 2: Steady-state FLN as a function of the size ℓ of region A (see Fig. 1), for $\ell \leq N/2$. The data are for the tight-binding chain with $N = 1000$ and $h = 1.1$, connected to two reservoirs with temperatures $T_L = 10$, $T_R = 15$ and chemical potentials $\mu_L = 1$, $\mu_R = 1.5$. Here we choose $\gamma = 0.2$ and $\Omega = 10$ for the spectral density [cf. (47)]. The inset shows the same data in logarithmic scale on the x-axis.

choose $\Omega = 10$ and $\gamma = 0.2$, so that we are in the weak-coupling regime. The various symbols in the figure correspond to results associated with different master equations. Provided that ℓ is sufficiently smaller than N, the FLN exhibits logarithmic scaling as a function of ℓ for all the three master equations. Even though the three approaches give different numerical results, due to the different approximations employed to derive them, the qualitative behavior of the FLN is the same. For the global Lindblad equation, the logarithmic scaling is compatible with what was established in Ref. [38], whereas it is not obvious for the Redfield and the ULE approaches.

Inspired by the results of Ref. [38], we now consider how $\mathscr{E}_F$ depends on the so-called chord length X_ℓ, which is defined as

$$X_\ell := \frac{N}{\pi} \sin\left(\frac{\pi \ell}{N}\right), \quad \ell = 1, \ldots, N. \tag{49}$$

In systems described by a CFT, the scaling of the entanglement entropy in the limit $N, \ell \to \infty$ depends on X_ℓ, and not on ℓ and N separately [66, 78]. Such a feature was also verified in ground states of spin chains described by the random singlet phase [79]. Moreover, one can show that the FLN between two complementary intervals in a globally pure state becomes the Rényi entropy of one of the intervals, which in CFTs exhibits a logarithmic scaling with the chord length [73]. Furthermore, the mutual information between A and B exhibits scaling as a function of X_ℓ [38].

In Fig. 3 we plot the steady-state FLN as a function of X_ℓ, using the same parameters of Fig. 2. Numerical data exhibit logarithmic scaling for all the three master equations, even though the prefactor of such a logarithmic growth is different in the three cases. This allows us to conclude that the logarithmic entanglement scaling observed in Ref. [38] for the global Lindblad equation holds true also in the Redfield and ULE approaches, at least for weak coupling and moderately large subsystem size ℓ.

However, it is important to stress that if $\mathscr{E}_F$ is a function of X_ℓ only, the data for different values of N should collapse on the same curve, at least in the thermodynamic

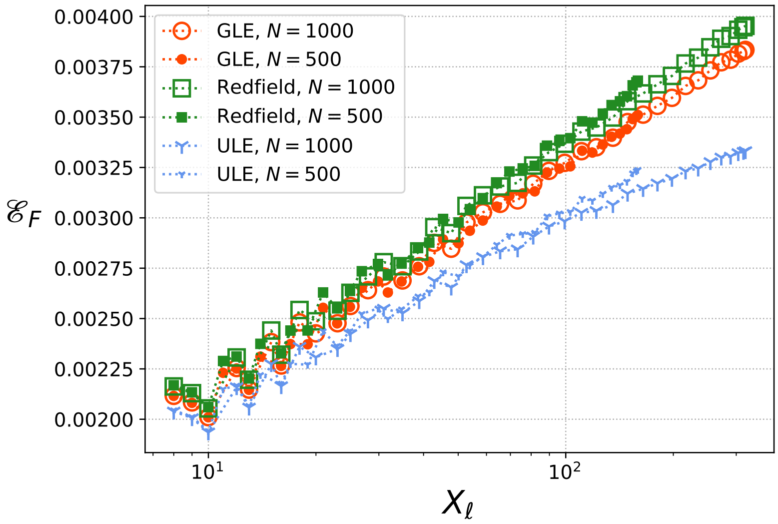

Figure 3: Steady-state FLN as a function of the chord length X_ℓ [cf. (49)]. Notice the logarithmic scale on the x-axis. The full symbols are the results for $N = 500$, while the empty ones are for $N = 1000$. The other parameters are the same as in Fig. 2.

limit $N, \ell \to \infty$. In Fig. 3 we report with the full symbols numerical data for $N = 500$. While we observe perfect scaling for the global Lindblad equation, the scenario is different for the Redfield and ULE approaches. For instance, the data obtained from the ULE for $N = 500$ and $N = 1000$ suggest that the collapse fails for the large interval sizes with $X_\ell \gtrsim 10^2$. Similar behavior occurs for the Redfield equation, even though the violations are significantly weaker. While such violations of scaling collapse could be attributed to finite-size effects, we will show in Sec. 5.3 that they rather signal a crossover to superlogarithmic scaling at asymptotically large X_ℓ.

Before proceeding, we investigate the behavior of the prefactor of the putative logarithmic scaling of $\mathscr{E}_F$. To this purpose, we fit the data in Fig. 3 with

$$\mathscr{E}_F = \widetilde{c} \ln(X_\ell) + b, \tag{50}$$

where $\widetilde{c}$ and b are the fitting parameters. In Fig. 4 we plot $\widetilde{c}$ as a function of T_R, for fixed $T_L = 1$. The two panels correspond to two different values of the coupling γ. For $\gamma = 0.2$ [panel (a)], $\widetilde{c}$ is similar for the three master equations. This is expected, since by construction the three approaches become equivalent in the limit $\gamma \to 0$. At $T_R \approx T_L$, $\widetilde{c}$ is larger, and it exhibits a decreasing trend upon increasing T_R, which is qualitatively similar to the behavior of the mutual information derived in Ref. [38]. Notice that, in principle, $\widetilde{c}$ could be obtained analytically for the global Lindblad equation by using the results of Refs. [38, 41]. Finally, Fig. 4 confirms that for $\gamma = 2$ [panel (b)] the three master equations yield significantly different behaviors for $\mathscr{E}_F$.

5.3 Violations of logarithmic scaling in the Redfield and the ULE approaches

Let us now investigate what happens by increasing the value of γ, thus exiting the weak-coupling regime. In Fig. 5 we plot the FLN $\mathscr{E}_F$ as a function of the chord length X_ℓ for several values of γ and μ_R, while keeping the remaining parameters as in Fig. 2. At weak coupling $\gamma = 0.2$ [panels (a) and (c)], the FLN exhibits a logarithmic increase, as expected, for both $\mu_R = 2$ and $\mu_R = 20$, and the three master equations lead to similar prefactors

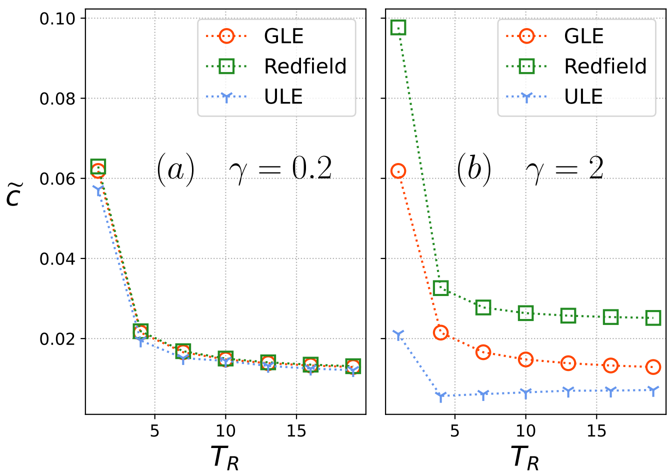

Figure 4: Prefactor $\widetilde{c}$ of the logarithmic scaling of the steady-state FLN [cf. Eq. (50)] as a function of T_R for fixed $T_L = 1$, calculated at $N = 1000$. Panels (a) and (b) are for two values of the system-bath interaction strength $\gamma = 0.2$ and $\gamma = 2$, respectively, while the other parameters are fixed as in Fig. 2.

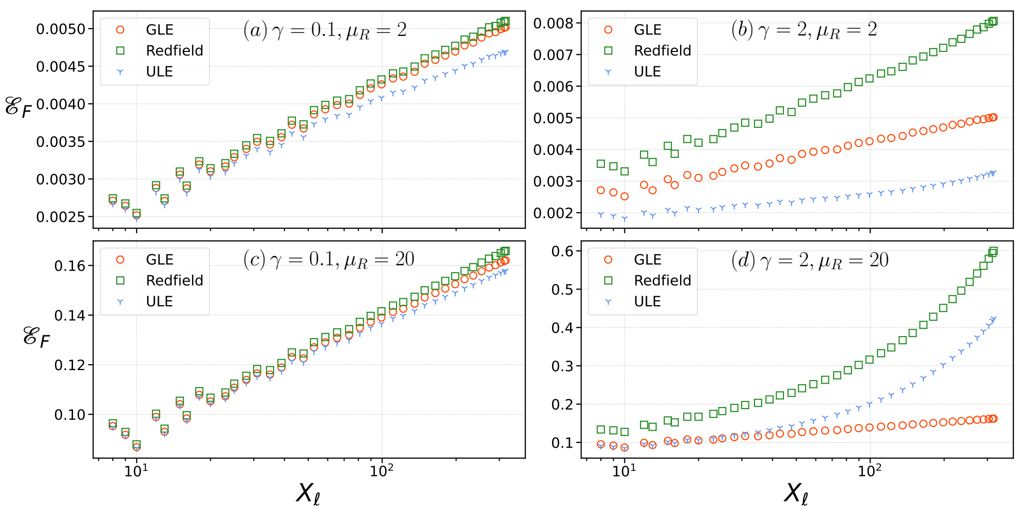

Figure 5: Steady-state FLN as a function of the chord length X_ℓ for different values of the coupling γ and the chemical potential of the right bath μ_R. The other parameters are fixed as in Fig. 2. Panels (a) and (c) show results in the weak-coupling regime for $\gamma = 0.1$ and $\mu_R = 2$ and $\mu_R = 20$, respectively. Panels (b) and (d) show results at strong coupling $\gamma = 2$ and $\mu_R = 2$ and $\mu_R = 20$, respectively.

for the logarithmic growth. The situation changes dramatically at stronger coupling $\gamma = 2$ [panels (b) and (d)]. For $\mu_R = 2$, we still observe an increase that is compatible with a logarithm, at least for $\ell \lesssim 200$. However, we notice a slight upward trend at large ℓ for both the ULE and the Redfield results, which suggests a violation of the logarithmic scaling at asympotically large ℓ. This becomes evident for $\mu_R = 20$ (see panel (d)). Now, the Redfield and ULE approaches clearly yield a superlogarithmic scaling of the FLN at large values of ℓ. This contrasts with the results of the global Lindblad equation (cirlces in panel (d)), which are compatible with a logarithmic growth at all values of γ and μ_R.

Finally, we should mention that, while our data exhibit superlogarithmic scaling for the FLN at large values of γ and μ_R, it is likely that the same behavior is present in the limit $\ell \to \infty$ for any γ, although the crossover length at which it starts to be visible presumably increases upon lowering γ. Unfortunaly, the chain sizes that are accessible with our numerics are not large enough to clarify this fact. Moreover, our results allow to conclude that the superlogarithmic growth is not related to the lack of complete positivity of the state, because it happens also for the ULE, which preserves complete positivity by construction. The superlogarithmic growth is likely due to the weak-coupling assumption in the Born-Markov approximation that is used to derive both the Redfield and the ULE [1, 48], and it signals the fact that the limit $\ell \to \infty$ and $\gamma \to 0$ do not commute.

6 Conclusions

We numerically investigated the steady-state entanglement in a tight-binding critical chain in contact with two thermal reservoirs at its edges. We showed that logarithmic entanglement scaling, as measured by the FLN, persists beyond the global Lindblad approach. Specifically, both the Redfield equation and the ULE yield logarithmic scaling for the steady-state negativity in the regime of weak system-bath coupling, in agreement with the global Lindblad approach [38]. However, upon increasing ℓ towards infinity or the coupling strength, both approaches give a superlogarithmic scaling for the negativity.

Our work opens several directions for future research. First, it is crucial to characterize the superlogarithmic entanglement scaling contribution. With the currently accessible system sizes we are not able to clarify whether the superlogarithmic scaling is power law or not. Moreover, it is important to understand whether such unusual entanglement scaling signals the breakdown of the Redfield and ULE equations, or it is a genuine physical effect.

It would be also interesting to characterize analytically the steadyt-state FLN. For the global Lindblad equation, this could be done by applying the results of Ref. [41], exploiting techniques based on the Fisher-Hartwig theorem [80–82]. This is more challenging for the Redfield equation and for the ULE, because the solutions of the Lyapunov equations (23) are not of the Toeplitz form, and a proper framework to extract the asymptotic properties of their spectrum is still missing. It would also interesting to understand whether the logarithmic entanglement scaling property survives in the presence of interactions. While this is a challenging task, it could be explored numerically by employing exact diagonalization methods. Finally, the presence of spurious superlogarithmic entanglement scaling indicates that caution is needed when trying to apply the global Lindblad and the Redfield equations, as well as the ULE to quantum many-body systems.

Acknowledgements

This study was carried out within the National Centre on HPC, Big Data and Quantum Computing - SPOKE 10 (Quantum Computing) and received funding from the European Union NextGenerationEU - National Recovery and Resilience Plan (NRRP) - MISSION 4 COMPONENT 2, INVESTMENT N. 1.4 - CUP N. I53C22000690001. This work has been supported by the project "Artificially devised many-body quantum dynamics in low dimensions - ManyQLowD", funded by the MIUR Progetti di Ricerca di Rilevante Interesse Nazionale (PRIN) Bando 2022 - grant 2022R35ZBF.

A Derivation of the pseudo-Lindblad form for the Redfield equation and the ULE

In this appendix we show how the Redfield equation (13) and the ULE (32) can be brought into the pseudo-Lindblad form (18). We split the derivation in two parts. First, in Secs. A.1 and A.2 we perform the transformation to normal-mode Majorana operators (17), showing that both equations lead to the same structure. In Sec. A.3 we discuss the pseudo-Lindblad form.

A.1 Redfield equation for Majorana operators

We first rewrite Eq. (13) in the Schrödinger picture as

$$\frac{d\rho}{dt} + i[H_S, \rho] = \sum_\alpha \int_0^\infty d\tau\, C_\alpha(\tau)[\widetilde{X}_\alpha(-\tau)\rho, X_\alpha] + \text{H.c.}, \tag{51}$$

where we used that $C_{\alpha\beta}$ in (15) is diagonal. Then, we express the operator X_α in Eq. (7a) using the transformation (11) to the normal modes d_k (cf. (11)), and the transformation (17) to corresponding Majorana operators m_k to obtain

$$X_\alpha = \sum_{k=1}^N \varphi_{\alpha,k}\left(d_k + d_k^\dagger\right) = \sqrt{2}\sum_{k=1}^N \varphi_{\alpha,k} m_{2k-1}. \tag{52}$$

The quantities $\varphi_{\alpha,k}$ are those defined in Eq. (21a). The interaction-picture form $\widetilde{X}_\alpha$ of X_α can be obtained through the Baker-Campbell-Hausdorff relation $e^{-iH_S t} d_k e^{iH_S t} = e^{iE_k t} d_k$. We obtain

$$\widetilde{X}_\alpha(-\tau) = \sum_{k=1}^N \varphi_{\alpha,k}\left(e^{iE_k\tau} d_k + e^{-iE_k\tau} d_k^\dagger\right) = \sqrt{2}\sum_{k=1}^N \varphi_{\alpha,k}[\cos(E_k\tau)m_{2k-1} - \sin(E_k\tau)m_{2k}].$$

Putting Eqs. (52) and (53) into Eq. (51), one then easily obtains

$$\frac{d\rho}{dt} + i[H_S, \rho] = \sum_{k,q=1}^N \left\{\mathcal{A}^r_{kq}[m_{2k-1}\rho, m_{2q-1}] + \mathcal{D}^r_{kq}[m_{2k}\rho, m_{2q-1}]\right\} + \text{H.c.}, \tag{53}$$

where $\mathcal{A}^r_{kq}$ and $\mathcal{D}^r_{kq}$ are defined in Eqs. (20). Here $\mathcal{A}^r$ and $\mathcal{D}^r$ depend on the function $\gamma(\omega)_\alpha$ (cf. (21b)), which are obtained from the $C_\alpha(\tau)$ in Eq. (15). Specifically, using the well-known identity

$$\int_0^\infty d\tau\, e^{ix\tau} = \pi\delta(x) + i\mathbb{P}\frac{1}{x}, \tag{54}$$

with $\mathbb{P}$ being the Cauchy principal value sign, we can rewrite Eq. (21b) as

$$\gamma_\alpha(\omega) = \pi \hat{C}_\alpha(\omega) + i\mathbb{P}\int_{-\infty}^{\infty} dx\, \frac{\hat{C}_\alpha(x)}{\omega - x}, \tag{55}$$

where $\hat{C}_\alpha(\omega) \coloneqq \int_{-\infty}^{\infty}(d\tau/2\pi)C_\alpha(\tau)e^{i\omega\tau}$ is the Fourier transform of $C_\alpha(\tau)$, given by

$$\hat{C}_\alpha(\omega) = \mathcal{J}_\alpha(-\omega)f_\alpha(-\omega) + \mathcal{J}_\alpha(\omega)[1 - f_\alpha(\omega)]. \tag{56}$$

A.2 Universal Lindblad Equation for Majorana operators

As for the Redfield equation, we start by reverting the interaction picture in Eq. (32). We find

$$\frac{d\rho}{dt} + i[H_S, \rho] = \sum_\alpha \int_{-\infty}^{\infty} d\tau \int_{-\infty}^{\infty} d\tau'\, \theta(\tau - \tau') \times g_\alpha(\tau) g_\alpha(-\tau')[\widetilde{X}_\alpha(\tau')\rho, \widetilde{X}_\alpha(\tau)] + \text{H.c.}. \tag{57}$$

After using Eq. (53) to write $\widetilde{X}_\alpha$ in terms of normal-mode Majorana operators, we obtain

$$\begin{aligned}\frac{d\rho}{dt} + i[H_S, \rho] = \sum_{k,q=1}^{N} \big\{ &\mathcal{A}^u_{kq}[m_{2k-1}\rho, m_{2q-1}] + \mathcal{B}^u_{kq}[m_{2k}\rho, m_{2q}] \\ &+ \mathcal{C}^u_{kq}[m_{2k-1}\rho, m_{2q}] + \mathcal{D}^u_{kq}[m_{2k}\rho, m_{2q-1}] \big\} + \text{H.c.},\end{aligned} \tag{58}$$

where

$$\mathcal{A}^u_{kq} = \sum_\alpha \varphi_{\alpha,k}\varphi_{\alpha,q} \int_{-\infty}^{\infty} d\tau \int_{-\infty}^{\infty} d\tau'\, \theta(\tau - \tau') \times g_\alpha(\tau) g_\alpha(-\tau') 2\cos\big(E_k\tau'\big)\cos(E_q\tau), \tag{59}$$

and the other coefficients $\mathcal{B}^u_{kq}$, $\mathcal{C}^u_{kq}$, and $\mathcal{D}^u_{kq}$ are obtained from $\mathcal{A}^u_{kq}$ by replacing $\cos(E_k\tau')\cos(E_q\tau)$ with, respectively, $\sin(E_k\tau')\sin(E_q\tau)$, $\cos(E_k\tau')\sin(E_q\tau)$, and $\sin(E_k\tau')\cos(E_q\tau)$. Notice the symmetries $[\mathcal{A}^u]^T = \mathcal{A}^u$, $[\mathcal{B}^u]^T = \mathcal{B}^u$, and $[\mathcal{C}^u]^T = -\mathcal{D}^u$. To recover Eqs. (35), let us introduce the function $\mathcal{I}_\alpha(\omega, \omega')$ as

$$\mathcal{I}_\alpha(\omega, \omega') \coloneqq \int_{-\infty}^{\infty} d\tau d\tau'\, \theta(\tau - \tau') g_\alpha(\tau) g_\alpha(-\tau') e^{i\omega\tau' + i\omega'\tau}. \tag{60}$$

By using Eq. (60) it is straightforward to obtain Eqs. (35).

Equation (36) for $\mathcal{I}_\alpha$ is derived as follows (see also Ref. [48]). First, we employ the relationship

$$\theta(\tau - \tau') = \frac{1 + \text{sgn}(\tau - \tau')}{2} \tag{61}$$

to split $\mathcal{I}_\alpha$ into two contributions as

$$\mathcal{I}_\alpha(\omega, \omega') = \mathcal{I}^R_\alpha(\omega, \omega') + i\,\mathcal{I}^I_\alpha(\omega, \omega'). \tag{62}$$

For the first one we have

$$\begin{aligned}\mathcal{I}^R_\alpha(\omega, \omega') &\equiv \frac{1}{2}\int_{-\infty}^{\infty} d\tau d\tau'\, g_\alpha(\tau) g_\alpha(-\tau') e^{i\omega\tau' + i\omega'\tau} \\ &= \frac{1}{2}(2\pi)^2 \hat{g}_\alpha(-\omega)\hat{g}_\alpha(\omega') = \pi\sqrt{\hat{C}_{\alpha\alpha}(-\omega)\hat{C}_{\alpha\alpha}(\omega')},\end{aligned} \tag{63}$$

where $\hat{g}_\alpha(\omega) := \frac{1}{2\pi}\int_{-\infty}^{\infty} d\tau\, g_\alpha(\tau)e^{i\omega\tau} = \sqrt{\hat{C}_\alpha(\omega)/2\pi}$ is the Fourier transform of $g_\alpha(\tau)$, and we used Eq. (33). For the second term in (62) we can now use the fact that $g_\alpha(\tau) = \int_{-\infty}^{\infty} dE\, \hat{g}_\alpha(E)e^{-iE\tau}$ to write

$$\begin{aligned}\mathcal{I}^I_\alpha(\omega,\omega') &= -\frac{i}{2}\int_{-\infty}^{\infty} d\tau d\tau' \,\mathrm{sgn}(\tau-\tau') \times g_\alpha(\tau)g_\alpha(-\tau')e^{i\omega\tau'+i\omega'\tau} \\ &= -\frac{i}{2}\int_{-\infty}^{\infty} dE dE'\,\mathcal{R}(\omega'-E,\omega+E')\hat{g}_\alpha(E)\hat{g}_\alpha(E'), \end{aligned} \tag{64}$$

where

$$\begin{aligned}\mathcal{R}(E,E') &:= \int_{-\infty}^{\infty} d\tau d\tau' \,\mathrm{sgn}(\tau-\tau')e^{iE\tau+iE'\tau'} \\ &= \int_{-\infty}^{\infty} d\tau \int_{-\infty}^{\tau} d\tau' \Big(e^{iE\tau+iE'\tau'} - e^{iE\tau'+iE'\tau}\Big). \end{aligned} \tag{65}$$

After the change of variable $\tau' = \tau - s$, we obtain

$$\mathcal{R}(E,E') = \int_{-\infty}^{\infty} d\tau e^{i(E+E')\tau} \int_0^{\infty} ds \Big(e^{-iE's} - e^{-iEs}\Big). \tag{66}$$

Using Eq. (54), this becomes

$$\mathcal{R}(E,E') = -4\pi i\delta(E+E')\mathbb{P}\frac{1}{E}. \tag{67}$$

After substituting Eq. (67) back into Eq. (64), and after performing the integration over E', we arrive at

$$\mathcal{I}^I_\alpha(\omega,\omega') = -2\pi\mathbb{P}\int_{-\infty}^{\infty} \frac{dE}{E}\hat{g}_\alpha(E-\omega)\hat{g}_\alpha(E+\omega'), \tag{68}$$

which is the same as Eq. (36). Equation (36) is somehow easier to evaluate numerically than (60).

A.3 Pseudo-Lindblad form of the Redfield equation and the ULE

In Sec. A.1 and Sec. A.2 we showed how the Redfield equation and the ULE can be rewritten using normal-mode Majorana operators in the form

$$\begin{aligned}\frac{d\rho}{dt} + i[H_S,\rho] = \sum_{k,q=1}^{N} \big\{ &\mathcal{A}_{kq}[m_{2k-1}\rho, m_{2q-1}] + \mathcal{B}_{kq}[m_{2k}\rho, m_{2q}] + \mathcal{C}_{kq}[m_{2k-1}\rho, m_{2q}] \\ &+ \mathcal{D}_{kq}[m_{2k}\rho, m_{2q-1}]\big\} + \text{H.c.}, \end{aligned} \tag{69}$$

where $\mathcal{A}\mapsto\mathcal{A}^r$, $\mathcal{D}\mapsto\mathcal{D}^r$, and $\mathcal{B},\mathcal{C}\mapsto 0$ for the Redfield case, while $\mathcal{A}\mapsto\mathcal{A}^u$, $\mathcal{B}\mapsto\mathcal{B}^u$, $\mathcal{C}\mapsto\mathcal{C}^u$, and $\mathcal{D}\mapsto -[\mathcal{C}^u]^T$ for the ULE case. We now derive a master equation in pseudo-Lindblad form starting from Eq. (69) with generic coefficients $\mathcal{A}_{kq}$, $\mathcal{B}_{kq}$, $\mathcal{C}_{kq}$, and $\mathcal{D}_{kq}$. First, we write the Hamiltonian as

$$H_S = -\frac{i}{2}\sum_{k,q=1}^{N} \delta_{kq}E_k(m_{2q}m_{2k-1} - m_{2q-1}m_{2k}), \tag{70}$$

where the presence of δ_{kq} reflects that the Hamiltonian is translation invariant. By using Eq. (70) in Eq. (69), one can easily verify that

$$\frac{d\rho}{dt} = \sum_{c,d=1}^{2N} \Big[V_{cd} m_c \rho m_d - W_{cd} m_d m_c \rho - W_{cd}^{\dagger} \rho m_d m_c \Big], \tag{71}$$

where V and W are $2N \times 2N$ complex matrices. The 2×2 blocks $\mathcal{V}_{kq}$ and $\mathcal{W}_{kq}$ associated with the entries $(2k-1, 2q-1)$, $(2k-1, 2q)$, $(2k, 2q-1)$, $(2k, 2q)$ of V and W are respectively given by

$$\mathcal{V}_{kq} = \begin{pmatrix} \mathcal{A}_{kq} + \mathcal{A}_{qk}^* & \mathcal{C}_{kq} + \mathcal{D}_{qk}^* \\ \mathcal{D}_{kq} + \mathcal{C}_{qk}^* & \mathcal{B}_{kq} + \mathcal{B}_{qk}^* \end{pmatrix}, \tag{72a}$$

$$\mathcal{W}_{kq} = \begin{pmatrix} \mathcal{A}_{kq} & \mathcal{C}_{kq} + \delta_{kq} E_k/2 \\ \mathcal{D}_{kq} - \delta_{kq} E_k/2 & \mathcal{B}_{kq} \end{pmatrix}. \tag{72b}$$

Note that $\mathcal{V}_{kq} = \mathcal{W}_{kq} + \mathcal{W}_{qk}^{\dagger}$, and therefore one has that $V = W + W^{\dagger}$. We now decompose W in its Hermitian and anti-Hermitian components as

$$M := \frac{W + W^{\dagger}}{2}, \quad L := \frac{W - W^{\dagger}}{2}. \tag{73}$$

This allows us to obtain the matrices L and M in Eq. (18). As it is clear from Eqs. (72), $M = V/2$. Moreover, the 2×2 block $\mathcal{L}_{kq}$ associated to L is

$$\mathcal{L}_{kq} = \frac{1}{2} \begin{pmatrix} \mathcal{A}_{kq} - \mathcal{A}_{qk}^* & \delta_{kq} E_k + \mathcal{C}_{kq} - \mathcal{D}_{qk}^* \\ -\delta_{kq} E_k + \mathcal{D}_{kq} - \mathcal{C}_{qk}^* & \mathcal{B}_{kq} - \mathcal{B}_{qk}^* \end{pmatrix}. \tag{74}$$

A straightforward computation can now be carried out to show that Eq. (71) coincides with Eq. (18).

References

[1] H.-P. Breuer and F. Petruccione, *The Theory of Open Quantum Systems*, Oxford University Press, doi:10.1093/acprof:oso/9780199213900.001.0001 (2002).

[2] A. Rivas and S. F. Huelga, *Open Quantum Systems: An Introduction*, Springer Berlin, Heidelberg, doi:10.1007/978-3-642-23354-8 (2011).

[3] F. Verstraete, M. Wolf and J. I. Cirac, *Quantum computation and quantum-state engineering driven by dissipation*, Nature Phys. **5**, 633 (2009), doi:10.1038/nphys1342.

[4] F. Binder *et al.*, eds., *Thermodynamics in the Quantum Regime*, Springer Cham, doi:10.1007/978-3-319-99046-0 (2019).

[5] Y. Cao *et al.*, *Quantum chemistry in the age of quantum computing*, Chem. Rev. **119**, 10856 (2019), doi:10.1021/acs.chemrev.8b00803.

[6] L. Amico, R. Fazio, A. Osterloh and V. Vedral, *Entanglement in many-body systems*, Rev. Mod. Phys. **80**, 517 (2008), doi:10.1103/RevModPhys.80.517.

[7] P. Calabrese, J. Cardy and B. Doyon, *Entanglement entropy in extended quantum systems*, J. Phys. A: Math. Theor. **42**, 500301 (2009), doi:10.1088/1751-8121/42/50/500301.

[8] J. Eisert, M. Cramer and M. B. Plenio, *Colloquim: Area laws for the entanglement entropy*, Rev. Mod. Phys. **82**, 277 (2010), doi:10.1103/RevModPhys.82.277.

[9] N. Laflorencie, *Quantum entanglement in condensed matter systems*, Phys. Rep. **646**, 1 (2016), doi:10.1016/j.physrep.2016.06.008.

[10] L. Aolita, F. de Melo and L. Davidovich, *Open-system dynamics of entanglement: A key issues review*, Rep. Prog. Phys. **78**, 042001 (2015), doi:10.1088/0034-4885/78/4/042001.

[11] P. Calabrese and J. Cardy, *Evolution of entanglement entropy in one-dimensional systems*, J. Stat. Mech. **2005**, P04010 (2005), doi:10.1088/1742-5468/2005/04/p04010.

[12] M. Fagotti and P. Calabrese, *Evolution of entanglement entropy following a quantum quench: Analytic results for the XY chain in a transverse magnetic field*, Phys. Rev. A **78**, 010306 (2008), doi:10.1103/PhysRevA.78.010306.

[13] V. Alba and P. Calabrese, *Entanglement and thermodynamics after a quantum quench in integrable systems*, PNAS **114**, 7947 (2017), doi:10.1073/pnas.170351611.

[14] V. Alba and P. Calabrese, *Entanglement dynamics after quantum quenches in generic integrable systems*, SciPost Phys. **4**, 17 (2018), doi:10.21468/SciPostPhys.4.3.017.

[15] V. Alba, B. Bertini, M. Fagotti, L. Piroli and P. Ruggiero, *Generalized-hydrodynamic approach to inhomogeneous quenches: correlations, entanglement and quantum effects*, J. Stat. Mech. **2021**, 114004 (2021), doi:10.1088/1742-5468/ac257d.

[16] K. Klobas and B. Bertini, *Entanglement dynamics in rule 54: Exact results and quasiparticle picture*, SciPost Phys. **11**, 107 (2021), doi:10.21468/SciPostPhys.11.6.107.

[17] B. Bertini, K. Klobas, V. Alba, G. Lagnese and P. Calabrese, *Growth of Rényi entropies in interacting integrable models and the breakdown of the quasiparticle picture*, Phys. Rev. X **12**, 031016 (2022), doi:10.1103/PhysRevX.12.031016.

[18] A. Coser, E. Tonni and P. Calabrese, *Entanglement negativity after a global quantum quench*, J. Stat. Mech. **2014**, P12017 (2014), doi:10.1088/1742-5468/2014/12/p12017.

[19] V. Alba and P. Calabrese, *Quantum information dynamics in multipartite integrable systems*, EPL **126**, 60001 (2019), doi:10.1209/0295-5075/126/60001.

[20] M. M. Wolf, F. Verstraete, M. B. Hastings and J. I. Cirac, *Area laws in quantum systems: Mutual information and correlations*, Phys. Rev. Lett. **100**, 070502 (2008), doi:10.1103/PhysRevLett.100.070502.

[21] V. Marić and M. Fagotti, *Universality in the tripartite information after global quenches*, Phys. Rev. B **108**, L161116 (2023), doi:10.1103/PhysRevB.108.L161116.

[22] B. Groisman, S. Popescu and A. Winter, *Quantum, classical, and total amount of correlations in a quantum state*, Phys. Rev. A **72**, 032317 (2005), doi:10.1103/PhysRevA.72.032317.

[23] G. Vidal and R. F. Werner, *Computable measure of entanglement*, Phys. Rev. A **65**, 032314 (2002), doi:10.1103/PhysRevA.65.032314.

[24] M. B. Plenio, *Logarithmic negativity: A full entanglement monotone that is not convex*, Phys. Rev. Lett. **95**, 090503 (2005), doi:10.1103/PhysRevLett.95.090503.

[25] J. Eisert, *Entanglement in quantum information theory*, Ph.D. thesis, University of Potsdam (2001).

[26] V. Alba and F. Carollo, *Spreading of correlations in Markovian open quantum systems*, Phys. Rev. B **103**, L020302 (2021), doi:10.1103/PhysRevB.103.L020302.

[27] F. Carollo and V. Alba, *Dissipative quasiparticle picture for quadratic Markovian open quantum systems*, Phys. Rev. B **105**, 144305 (2022), doi:10.1103/PhysRevB.105.144305.

[28] V. Alba and F. Carollo, *Hydrodynamics of quantum entropies in Ising chains with linear dissipation*, J. Phys. A: Math. Theor. **55**, 074002 (2022), doi:10.1088/1751-8121/ac48ec.

[29] S. Murciano, P. Calabrese and V. Alba, *Symmetry-resolved entanglement in fermionic systems with dissipation*, J. Stat. Mech. **2023**, 113102 (2023), doi:10.1088/1742-5468/ad0224.

[30] F. Caceffo, S. Murciano and V. Alba, *Entangled multiplets, asymmetry, and quantum Mpemba effect in dissipative systems*, J. Stat. Mech. **2024**, 063103 (2024), doi:10.1088/1742-5468/ad4537.

[31] V. Alba and F. Carollo, *Logarithmic negativity in out-of-equilibrium open free-fermion chains: An exactly solvable case*, SciPost Phys. **15**, 124 (2023), doi:10.21468/SciPostPhys.15.3.124.

[32] F. Caceffo and V. Alba, *Fate of entanglement in quadratic Markovian dissipative systems*, URL `https://arxiv.org/abs/2406.15328`, Unpublished (2024), `2406.15328`.

[33] V. Alba and F. Carollo, *Noninteracting fermionic systems with localized losses: Exact results in the hydrodynamic limit*, Phys. Rev. B **105**, 054303 (2022), doi:10.1103/PhysRevB.105.054303.

[34] V. Alba, *Unbounded entanglement production via a dissipative impurity*, SciPost Phys. **12**, 11 (2022), doi:10.21468/SciPostPhys.12.1.011.

[35] F. Caceffo and V. Alba, *Entanglement negativity in a fermionic chain with dissipative defects: exact results*, J. Stat. Mech. **2023**, 023102 (2023), doi:10.1088/1742-5468/acb429.

[36] S. Frankel and M. Goldstein, *Entanglement measures in a nonequilibrium steady state: Exact results in one dimension*, SciPost Phys. **11**, 085 (2021), doi:10.21468/SciPostPhys.11.4.085.

[37] S. Fraenkel and M. Goldstein, *Extensive long-range entanglement at finite temperature from a nonequilibrium bias*, Phys. Rev. B **110**, 035149 (2024), doi:10.1103/PhysRevB.110.035149.

[38] A. D'Abbruzzo, V. Alba and D. Rossini, *Logarithmic entanglement scaling in dissipative free-fermion systems*, Phys. Rev. B **106**, 235149 (2022), doi:10.1103/PhysRevB.106.235149.

[39] G. T. Landi, D. Poletti and G. Schaller, *Nonequilibrium boundary-driven quantum systems: Models, methods, and properties*, Rev. Mod. Phys. **94**, 045006 (2022), doi:10.1103/RevModPhys.94.045006.

[40] P. Ribeiro, *Steady-state properties of a nonequilibrium Fermi gas*, Phys. Rev. B **96**, 054302 (2017), doi:10.1103/PhysRevB.96.054302.

[41] V. Eisler, *Entanglement negativity in a nonequilibrium steady state*, Phys. Rev. B **107**, 075157 (2023), doi:10.1103/PhysRevB.107.075157.

[42] A. D'Abbruzzo and D. Rossini, *Self-consistent microscopic derivation of Markovian master equations for open quadratic quantum systems*, Phys. Rev. A **103**, 052209 (2021), doi:10.1103/PhysRevA.103.052209.

[43] A. G. Redfield, *The theory of relaxation processes*, In *Advances in Magnetic Resonance*, pp. 1–32. Academic Press, doi:10.1016/B978-1-4832-3114-3.50007-6 (1965).

[44] R. Dümcke and H. Spohn, *The proper form of the generator in the weak coupling limit*, Physik B **34**, 419 (1979), doi:10.1007/BF01325208.

[45] G. Schaller and T. Brandes, *Preservation of positivity by dynamical coarse graining*, Phys. Rev. A **78**, 022106 (2008), doi:10.1103/PhysRevA.78.022106.

[46] A. Rivas, *Refined weak-coupling limit: Coherence, entanglement, and non-Markovianity*, Phys. Rev. A **95**, 042104 (2017), doi:10.1103/PhysRevA.95.042104.

[47] D. Farina and V. Giovannetti, *Open-quantum-system dynamics: Recovering positivity of the redfield equation via the partial secular approximation*, Phys. Rev. A **100**, 012107 (2019), doi:10.1103/PhysRevA.100.012107.

[48] F. Nathan and M. S. Rudner, *Universal Lindblad equation for open quantum systems*, Phys. Rev. B **102**, 115109 (2020), doi:10.1103/PhysRevB.102.115109.

[49] D. Davidović, *Geometric-arithmetic master equation in large and fast open quantum systems*, J. Phys. A: Math. Theor. **55**, 455301 (2022), doi:10.1088/1751-8121/ac9f30.

[50] H. Wichterich and M. J. Henrich and H.-P. Breuer and J. Gemmer and M. Michel, *Modeling heat transport through completely positive maps*, Phys. Rev. E **76**, 031115 (2007), doi:10.1103/PhysRevE.76.031115.

[51] A. Gordon and D. Majer, *Coherent transport in semiconductor heterostructures: A phenomenological approach*, Phys. Rev. B **80**, 195317 (2009), doi:10.1103/PhysRevB.80.195317.

[52] G. Kiršanskas and M. Franckié and A. Wacker, *Phenomenological position and energy resolving Lindblad approach to quantum kinetics*, Phys. Rev. B **97**, 035432 (2018), doi:10.1103/PhysRevB.97.035432.

[53] E. Kleinherbers and N. Szpak and J. König and R. Schützhold, *Relaxation dynamics in a Hubbard dimer coupled to fermionic baths: Phenomenological description and its microscopic foundation*, Phys. Rev. B **101**, 125131 (2020), doi:10.1103/PhysRevB.101.125131.

[54] A. D'Abbruzzo, V. Cavina and V. Giovannetti, *A time-dependent regularization of the Redfield equation*, SciPost Phys. **15**, 117 (2023), doi:10.21468/SciPostPhys.15.3.117.

[55] A. D'Abbruzzo, D. Farina and V. Giovannetti, *Recovering complete positivity of non-Markovian quantum dynamics with Choi-proximity regularization*, Phys. Rev. X **14**, 031010 (2024), doi:10.1103/PhysRevX.14.031010.

[56] G. McCauley *et al.*, *Accurate Lindblad-form master equation for weakly damped quantum systems across all regimes*, npj Quantum Inf. **6**, 74 (2020), doi:10.1038/s41534-020-00299-6.

[57] E. Mozgunov and D. Lidar, *Completely positive master equation for arbitrary driving and small level spacing*, Quantum **4**, 227 (2020), doi:10.22331/q-2020-02-06-227.

[58] P. P. Potts, A. A. S. Kalaee and A. Wacker, *A thermodynamically consistent Markovian master equation beyond the secular approximation*, New J. Phys. **23**, 123013 (2021), doi:10.1088/1367-2630/ac3b2f.

[59] T. Becker, L.-N. Wu and A. Eckardt, *Lindbladian approximation beyond ultraweak coupling*, Phys. Rev. E **104**, 014110 (2021), doi:10.1103/PhysRevE.104.014110.

[60] A. Trushechkin, *Unified Gorini-Kossakowski-Lindblad-Sudarshan quantum master equation beyond the secular approximation*, Phys. Rev. A **103**, 062226 (2021), doi:10.1103/PhysRevA.103.062226.

[61] T. Prosen and B. Žunkovič, *Exact solution of Markovian master equations for quadratic Fermi systems: thermal baths, open XY spin chains and non-equilibrium phase transition*, New J. Phys. **12**, 025016 (2010), doi:10.1088/1367-2630/12/2/025016.

[62] P. Ribeiro and V. R. Vieira, *Non-Markovian effects in electronic and spin transport*, Phys. Rev. B **92**, 100302 (2015), doi:10.1103/PhysRevB.92.100302.

[63] H. Ng, *Decoherence of interacting Majorana modes*, Sci. Rep. **5**, 12530 (2015), doi:10.1038/srep12530.

[64] M. Cirio and P.-C. Kuo and Y.-N. Chen and F. Nori and N. Lambert, *Canonical derivation of the fermionic influence superoperator*, Phys. Rev. B **105**, 035121 (2022), doi:10.1103/PhysRevB.105.035121.

[65] E. Lieb, T. Schultz and D. Mattis, *Two soluble models of an antiferromagnetic chain*, Ann. Phys. **16**, 407 (1961), doi:10.1016/0003-4916(61)90115-4.

[66] P. Di Francesco, P. Mathieu and D. Sénéchal, *Conformal Field Theory*, Springer-Verlag, New York, doi:10.1007/978-1-4612-2256-9 (1997).

[67] A. R. Its, B.-Q. Jin and V. E. Korepin, *Entanglement in the XY spin chain*, J. Phys. A: Math. Gen. **38**, 2975 (2005), doi:10.1088/0305-4470/38/13/011.

[68] Z. Gajić and M. T. J. Qureshi, eds., *Lyapunov Matrix Equation in System Stability and Control*, Academic Press (1995).

[69] A. Purkayastha, *Lyapunov equation in open quantum systems and non-Hermitian physics*, Phys. Rev. A **105**, 062204 (2022), doi:10.1103/PhysRevA.105.062204.

[70] T. Barthel and V. Zhang, *Solving quasi-free and quadratic Lindblad master equations for open fermionic and bosonic systems*, J. Stat. Mech. **2022**, 113101 (2022), doi:10.1088/1742-5468/ac8e5c.

[71] K. Audenaert, J. Eisert, M. B. Plenio and R. F. Werner, *Entanglement properties of the harmonic chain*, Phys. Rev. A **66**, 042327 (2002), doi:10.1103/PhysRevA.66.042327.

[72] V. Eisler and Z. Zimborás, *On the partial transpose of fermionic Gaussian states*, New J. Phys. **17**, 053048 (2015), doi:10.1088/1367-2630/17/5/053048.

[73] H. Shapourian, K. Shiozaki and R. Shinsei, *Partial time-reversal transformation and entanglement negativity in fermionic systems*, Phys. Rev. B **95**, 165101 (2017), doi:10.1103/PhysRevB.95.165101.

[74] J. Eisert, V. Eisler and Z. Zimborás, *Entanglement negativity bounds for fermionic Gaussian states*, Phys. Rev. B **97**, 165123 (2018), doi:10.1103/PhysRevB.97.165123.

[75] H. Shapourian and R. Shinsei, *Entanglement negativity of fermions: Monotonicity, separability criterion, and classification of few-mode states*, Phys. Rev. A **99**, 022310 (2019), doi:10.1103/PhysRevA.99.022310.

[76] G. Camilo, G. T. Landi and S. Eliëns, *Strong subadditivity of the Rényi entropies for bosonic and fermionic Gaussian states*, Phys. Rev. B **99**, 045155 (2019), doi:10.1103/PhysRevB.99.045155.

[77] R. H. Bartels and G. W. Stewart, *Solution of the matrix equation $AX + XB = C$*, Comm. ACM **15**, 820 (1972), doi:10.1145/361573.361582.

[78] P. Calabrese and J. Cardy, *Entanglement entropy and conformal field theory*, J. Phys. A: Math. Theor. **42**, 504005 (2009), doi:10.1088/1751-8113/42/50/504005.

[79] M. Fagotti, P. Calabrese and J. E. Moore, *Entanglement spectrum of random-singlet quantum critical points*, Phys. Rev. B **83**, 045110 (2011), doi:10.1103/PhysRevB.83.045110.

[80] M. E. Fisher and R. E. Hartwig, *Toepliz Determinants: Some Applications, Theorems, and Conjectures*, In *Advances in Chemical Physics*, pp. 333–353. John Wiley & Sons, Ltd., doi:10.1002/9780470143605.ch18 (1969).

[81] E. L. Basor and C. A. Tracy, *The Fisher-Hartwig conjecture and generalizations*, Physica A **177**, 167 (1991), doi:10.1016/0378-4371(91)90149-7.

[82] E. L. Basor and K. E. Morrison, *The Fisher-Hartwig conjecture and Toeplitz eigenvalues*, Linear Algebra Appl. **202**, 129 (1994), doi:10.1016/0024-3795(94)90187-2.